

Investigation of Carotenoid Radical Cations and Triplet States by Laser Flash Photolysis and Time-Resolved Resonance Raman Spectroscopy: Observation of Competitive Energy and Electron Transfer

J. H. Tinkler,[†] S. M. Tavender,[‡] A. W. Parker,[‡] D. J. McGarvey,^{*,†}
L. Mulroy,[†] and T. G. Truscott[†]

Contribution from the Chemistry Department, Keele University, Keele ST5 5BG, England, U.K., and Lasers for Science Facility, Rutherford Appleton Laboratory, CCLRC Chilton, Didcot, Oxfordshire OX11 0QX, England, U.K.

Received September 18, 1995[⊗]

Abstract: The first nanosecond time-resolved resonance Raman study of carotenoid radical cations is reported for the polyenes septapreno- β -carotene and 7,7'-dihydro- β -carotene. In addition, previously unreported resonance Raman spectra of the ground and triplet states of these molecules are reported. The radical cations were generated following electron transfer quenching of triplet 1-nitronaphthalene in methanol and Triton X-100 micelles. The quenching of triplet 1-nitronaphthalene by these carotenoids involves solvent-dependent competition between energy transfer and electron transfer, and for both carotenoids, estimates are given for the efficiencies of these two processes in methanol and hexane. The resonance Raman spectra of septapreno- β -carotene ground and triplet states are consistent with spectra reported previously for other carotenoids. However, the resonance Raman spectrum of the triplet state of 7,7'-dihydro- β -carotene displays an intensity profile not found in the triplet spectra of other carotenoids. In addition, the resonance Raman spectrum of the radical cation of 7,7'-dihydro- β -carotene is quite distinct from that of septapreno- β -carotene. These observations are attributed to differences in electronic structure arising from septapreno- β -carotene having an odd number of conjugated double bonds while 7,7'-dihydro- β -carotene, unusually, has an even number.

Introduction

Carotenoids are present in the chloroplasts of green plants^{1,2} and serve to protect the photosynthetic system from photodynamic (photo-oxidative) damage. This is achieved by quenching of chlorophyll triplet states, thereby precluding formation of singlet oxygen, and possibly by direct quenching of singlet oxygen. Carotenoids also function as accessory light-harvesting pigments in the antenna systems of photosynthetic organisms, absorbing light energy in the spectral region where chlorophyll absorption is weak. In addition, they may participate in the photosynthetic electron transfer chain with formation of carotenoid radical cations. Although there is no direct evidence that carotenoid radical cations are involved in normal photosynthetic electron flow, Mathis and co-workers^{3,4} have observed absorption changes following photoexcitation of chloroplasts that they attribute to a carotene radical cation at the photosystem II reaction center. Similarly, Barber *et al.*⁵ have observed the formation of carotene radical cations in "blocked" reaction centers.

Light-initiated electron transfer across membranes is of interest in the development of artificial photosynthetic systems and again the role of carotene radical cations may be important.

For example, in a series of elegant studies Gust, Moore, and co-workers⁶ synthesized a series of triad molecules in which a porphyrin (P) is covalently linked on one side to a carotenoid (Car) and, on the other, to a quinone (Q). This model of the key feature of photosynthetic reaction centers shows electron transfer from the porphyrin to the quinone following the absorption of light, with a second electron transfer then "repairing" the porphyrin radical cation and producing a final charge-separated system involving the carotene radical cation and the quinone radical anion (Car^{•+}–P–Q^{•-}). This suggests that carotenoid radical cations may play an integral part of the electron transfer system in photosynthesis.

Of particular current interest is the fact that carotenoids are known to be lipid-soluble antioxidants capable of quenching singlet oxygen and free radicals. Several epidemiological studies have established a correlation between β -carotene dietary supplementation and a reduced risk of serious diseases such as cancer,^{7–10} atherosclerosis, and possibly age-related macular degeneration.¹¹ Such radical scavenging would be expected to lead to production of carotenoid radical cations, and thus, the study of carotenoid radicals is of considerable importance. Indeed, in a recent paper,¹² we have shown that lycopene (the

[†] Keele University.

[‡] Rutherford Appleton Laboratory.

[⊗] Abstract published in *Advance ACS Abstracts*, January 15, 1996.

(1) Goedheer, J. C. *Ann. Rev. Plant Physiol.* **1972**, *23*, 87.

(2) Chessin, M.; Livingston, R.; Truscott, T. G. *Trans. Faraday Soc.* **1966**, *62*, 1519.

(3) Mathis, P.; Rutherford, A. W. *Biochem. Biophys. Acta* **1984**, *767*, 217.

(4) Schenck, C. C.; Diner, B.; Mathis, P.; Satoh, K. *Biochim. Biophys. Acta* **1982**, *680*, 216.

(5) Telfer, A.; De Las Rivas, J.; Barber, J. *Biochem. Biophys. Acta* **1991**, *1060*, 106.

(6) Moore, T. A.; Gust, D.; Mathis, P.; Mialocq, J. C.; Chachaty, C.; Bensasson, R. V.; Land, E. J.; Doizi, D.; Liddell, P. A.; Lehman, W. R.; Nemeth, G. A.; Moore, A. L. *Nature (London)* **1984**, *307*, 630.

(7) Mathews-Roth, M. M.; Krinsky, N. I. *Photochem. Photobiol.* **1985**, *42*, 35.

(8) Mathews-Roth, M. M.; Krinsky, N. I. *Photochem. Photobiol.* **1987**, *46*, 507.

(9) Epstein, J. H. *Photochem. Photobiol.* **1977**, *25*, 211.

(10) Menkes, M. S.; Comstock, G. W.; Vuilleumier, J. P.; Helsing, K. J.; Rider, A. A.; Brookmeyer, R. *New England J. Med.* **1986**, *315*, 1250.

(11) Schalch, W. *Free Radicals and Ageing*; Emerit, I., Chance, B., Eds.; Birkhauser Verlag: Switzerland, 1992; p 280.

(12) Bohm, F.; Tinkler, J. H.; Truscott, T. G. *Nature Med.* **1995**, *1*, 98.

red pigment in tomatoes) is considerably more effective than β -carotene in protecting human lymphocyte cells against damage by the NO_2 radical, such protection being associated with the formation of the respective carotenoid radical cations.

Resonance Raman spectroscopy has provided structural information on the ground, excited singlet, and triplet states of carotenoids,^{13–16} all of which have strong electronic absorption bands in the visible region. However, the principal electronic absorption bands of carotenoid radical cations are located in the less accessible near-infrared region (750–950 nm), and consequently, resonance Raman studies have been limited by the availability of sensitive near-infrared detectors. In this paper we report, for the first time, the time-resolved resonance Raman (TR^3) spectra of the radical cations of 7,7'-dihydro- β -carotene (77DH) and septapreno- β -carotene (SEPT) formed in methanol and detergent micelles by photoinduced electron transfer to the triplet state of 1-nitronaphthalene (NN). In addition, we report the observation of competitive energy and electron transfer during quenching of the triplet state of NN ($^3\text{NN}^*$) by 77DH and SEPT in methanol. The structures of 77DH and SEPT are given in Figure 1.

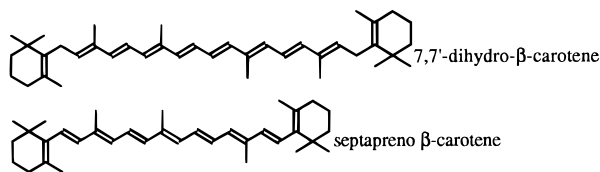


Figure 1. Structures of 77DH and SEPT.

Experimental Section

Materials. Septapreno- β -carotene and 7,7'-dihydro- β -carotene were supplied by Hoffmann-La Roche and stored in the dark at $-20\text{ }^\circ\text{C}$ under nitrogen; 1-nitronaphthalene (BDH) was recrystallized from ethanol; biphenyl (BDH) was recrystallized twice from ethanol; Triton X-100 (TX-100, Fluka), hexane, methanol (Aldrich, spectrophotometric grade), and benzene (Romil) were used as received.

Instrumentation. Kinetic absorption measurements employed the third harmonic (355 nm) of a Spectron Nd:YAG laser as the excitation source and a 250 W xenon arc lamp (Kratos) as the analyzing source. The 355 nm beam was attenuated using neutral density filters such that the laser intensity at the sample was typically $\sim 10\text{ mJ cm}^{-2}$. The sample cells were either a $2 \times 2 \times 10\text{ mm}$ quartz capillary flow cell (analyzing optical pathlength, 10 mm) or a $10 \times 10\text{ mm}$ quartz cuvette fitted with a vacuum tap. For measurements in the UV–visible region, an Applied Photophysics $f/3.4$ grating monochromator coupled to a Hamamatsu R928 photomultiplier tube was used. Near-infrared measurements employed a Bausch and Lomb monochromator and silicon photodiode detector. The transient absorption traces were fed to a Tektronix 2432A digital oscilloscope and the data transferred to an IBM-compatible PC via a GPIB interface.

Time-resolved resonance Raman measurements employed a pair of excimer (Lumonics Hyperex 460) pumped dye lasers (Lambda Physik, FL3002) operating at 388 nm/355 nm (pump wavelengths, 1.5 mJ pulse $^{-1}$; beam diameter at sample, $\sim 100\text{ }\mu\text{m}$) and 760 nm/485 nm (probe wavelengths, 0.5 mJ pulse $^{-1}$; beam diameter at sample, $\sim 100\text{ }\mu\text{m}$). The operating frequency was 20 Hz, and the spectra were typically acquired for 10–30 min. The delay between pump and probe pulses was 2 μs and was controlled by a Stanford DG535 pulse generator. The spectrograph used for resonance Raman measurements of the radical cations was a Spectra-Pro 500 (PI) with Rayleigh light rejection using a holographic notch filter. The ground state resonance

Raman spectra were obtained by c.w. excitation using an argon-ion laser (Coherent Innova 90) at 457.6 nm (laser power, 0.5 W; beam diameter at sample, $\sim 100\text{ }\mu\text{m}$). The spectrograph used for ground state and triplet state resonance Raman measurements was a triple monochromator (Spex Triplemate) as described previously.¹⁷ The detector used throughout was a thinned, back-illuminated liquid nitrogen cooled CCD camera (Princeton Instruments LN/CCD-1024TKB) with a 1024×1024 detector chip controlled by a model ST-130 controller interfaced to CSMA software. To minimize photodegradation, samples were flowed through a quartz capillary (diameter, 2.5 mm) at a rate of $\sim 5\text{ cm}^3\text{ min}^{-1}$.

Methods. For hexane, methanol, and micellar solutions, the carotenoid and 1-nitronaphthalene concentrations were $\sim 2 \times 10^{-5}$ and $\sim 10^{-3}\text{ mol dm}^{-3}$, respectively. The solutions were deoxygenated by bubbling with oxygen-free nitrogen (B.O.C., White Spot Grade). Micellar solutions were prepared by mixing a carbon tetrachloride solution of carotenoid and 1-nitronaphthalene with neat TX-100. The solution was then rotary evaporated ($\sim 40\text{ }^\circ\text{C}$) to remove the solvent, leaving a film of carotenoid and NN in TX-100. The film was then solubilized in distilled water such that the detergent concentration was 2% w/v.

Results and Discussion

1. Kinetic Absorption Studies. The use of aromatic nitro compounds in studies of photoinduced electron transfer is relatively rare and is due principally to the very short excited state lifetimes exhibited by these molecules. Excited singlet state lifetimes are of picosecond duration due to rapid intersystem crossing facilitated by the proximity of $n\pi^*$ to $\pi\pi^*$ states and to charge transfer (CT) mediated internal conversion. Similarly, the triplet states of aromatic nitro compounds are relatively short lived, particularly so for nitrobenzenes, and have a tendency to abstract hydrogen atoms from the solvent because of their $n\pi^*$ character. In the case of nitronaphthalenes however the triplet state lifetimes are considerably longer, particularly in polar solvents where the triplet is better described as a CT state than an $n\pi^*$ state.¹⁸ The half-wave reduction potential ($E(A/A^{\bullet-})$) of 1-nitronaphthalene is -0.98 V (vs SCE),¹⁹ which is comparable with that of 9,10-dicyanoanthracene, a well-known excited state electron acceptor.

In methanol, nanosecond (355 nm) laser excitation of NN produces $^3\text{NN}^*$, which under our experimental conditions decays by first-order kinetics with a lifetime of $\sim 12\text{ }\mu\text{s}$. The triplet lifetime in methanol, as expected, is longer than the lifetime reported previously¹⁸ for $^3\text{NN}^*$ in ethanol ($\sim 5\text{ }\mu\text{s}$) since ethanol is a better hydrogen atom donor than methanol. The triplet state absorption spectrum of NN in methanol is shown in Figure 2 and exhibits two main peaks in the visible region at ~ 400 and 580 nm . This spectrum is similar to the spectrum reported previously by Capellos and Porter¹⁸ for $^3\text{NN}^*$ in ethanol.

In hexane the increased $n\pi^*$ character of $^3\text{NN}^*$ results in a significantly shorter triplet state lifetime of $\sim 1\text{ }\mu\text{s}$, in good agreement with the value of $0.93\text{ }\mu\text{s}$ reported previously¹⁸ for this solvent. In addition, the absorption spectrum of $^3\text{NN}^*$ is shifted to shorter wavelengths with the principal absorption bands appearing at ~ 380 and $\sim 550\text{ nm}$, respectively (see Figure 2). This contrasts somewhat with the findings of Capellos and Porter,¹⁸ who report an absorption maximum at 525 nm for $^3\text{NN}^*$ in hexane. However, their spectrum relies on only a few widely-spaced data points (every 25 nm) which may explain the discrepancy.

(13) Dallinger, R. F.; Farquharson, S.; Woodruff, W. H.; Rodgers, M. A. *J. Am. Chem. Soc.* **1981**, *103*, 7433.

(14) Hashimoto, H.; Koyama, Y. *J. Phys. Chem.* **1988**, *92*, 2101.

(15) Koyama, Y.; Mukai, Y. *Biomolecular Spectroscopy*; J. Wiley & Sons: New York, 1993; Part B.

(16) Conn, P. F.; Haley, J.; Lambert, C. R.; Truscott, T. G.; Parker, A. W. *J. Chem. Soc., Faraday Trans.* **1993**, *89*, 1753.

(17) Vauthey, E.; Phillips, D.; Parker, A. W. *J. Phys. Chem.* **1992**, *96*, 7356.

(18) Capellos, C.; Porter, G. *J. Chem. Soc., Faraday Trans. 2* **1974**, *70*, 1159.

(19) Murov, S. L.; Carmichael, I.; Hug, G. L. *Handbook of Photochemistry*, 2nd Ed.; Marcel Dekker, Inc.: New York, 1993.

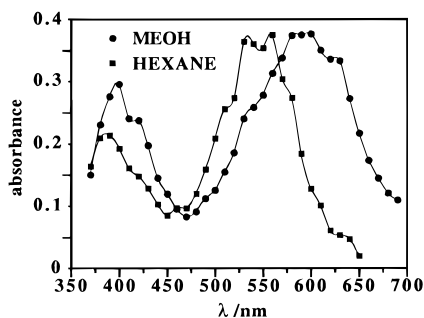


Figure 2. Triplet state absorption spectra of NN in hexane and methanol.

Following 355 nm laser excitation of hexane or methanol solutions of NN containing 77DH or SEPT, $^3\text{NN}^*$ is quenched by the carotenoid at rates approaching diffusion control. In hexane, the quenching proceeds exclusively (see later) by exchange energy transfer to produce the carotenoid triplet state observed via the triplet absorption maxima at 476 nm ($^3\text{77DH}^*$) and 475 nm ($^3\text{SEPT}^*$), respectively. No evidence of any other photoproducts was observed.

In methanol, however, quenching of $^3\text{NN}^*$ by carotenoid leads not only to formation of the carotenoid triplet state but also to the formation of a longer-lived species absorbing in the near-infrared region ($\lambda_{\text{max}} = 760$ and 820 nm for 77DH and SEPT, respectively; see Figures 3 and 4) which, by comparison with published spectra,²⁰ is attributed to the carotenoid radical cation. These observations imply the operation of electron transfer quenching in competition with exchange energy transfer as illustrated by Scheme 1.

Scheme 1

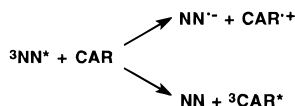


Figure 4 shows the kinetic absorption profiles observed at the respective λ_{max} for $^3\text{NN}^*$, $^3\text{77DH}^*$, and $^3\text{77DH}^{\cdot+}$ following 355 nm laser excitation of NN in methanol containing $\sim 2 \times 10^{-5}$ mol dm⁻³ 77DH. The kinetic traces show clearly the $^3\text{NN}^*$ decay with concomitant formation of $^3\text{77DH}^*$ and $^3\text{77DH}^{\cdot+}$. The NN radical anion ($\text{NN}^{\cdot-}$), which is expected to be produced via the electron transfer channel of Scheme 1, could not, however, be detected in these solutions. The visible absorption spectrum of this radical has been obtained in dimethylformamide using electrochemical methods²¹ and shows a peak around 660 nm with a relatively low absorption coefficient ($\epsilon_{\text{max}} = 2000$ dm³ mol⁻¹ cm⁻¹). The fact that we do not observe $\text{NN}^{\cdot-}$ in the red region of the spectrum may be due to its low absorption intensity at these wavelengths.

There are relatively few well-characterized examples of photochemical systems that exhibit competitive energy and electron transfer,²² and so it is of interest to determine the relative importance of the two channels for the $^3\text{NN}^*/\text{carotenoid}$ system. The efficiencies of energy and electron transfer (Φ_{en} and Φ_{el} , respectively) can be estimated from kinetic absorption data using the molar absorption coefficients of the participating species. The relevant photophysical data for NN, 77DH, and SEPT are summarized in Table 1.

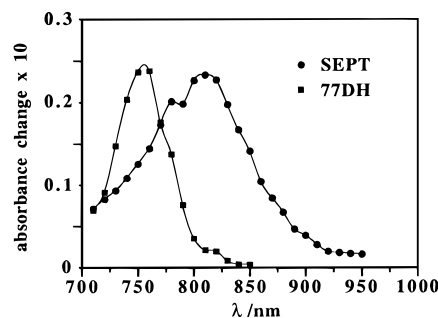


Figure 3. Absorption spectra of $^3\text{77DH}^{\cdot+}$ and $^3\text{SEPT}^{\cdot+}$ in methanol obtained following nanosecond 355 nm laser excitation of a solution of NN containing $\sim 2 \times 10^{-5}$ mol dm⁻³ carotenoid.

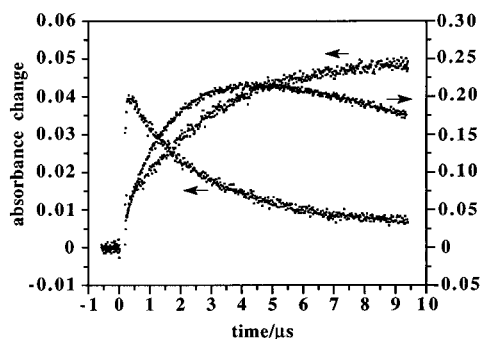


Figure 4. Kinetic absorption traces demonstrating competitive energy and electron transfer following nanosecond 355 nm laser excitation of a methanol solution of NN containing $\sim 2 \times 10^{-5}$ mol dm⁻³ 77DH. The traces show respectively the decay of $^3\text{NN}^*$ at 590 nm (left axis), the growth of $^3\text{77DH}^{\cdot+}$ at 750 nm (left axis), and the growth and decay of $^3\text{77DH}^*$ at 476 nm (right axis).

Unfortunately, no absorption coefficients are available for $^3\text{77DH}^{\cdot+}$ and $^3\text{SEPT}^{\cdot+}$ and so estimates of Φ_{en} and Φ_{el} are based on triplet state data only, with the assumption that $\Phi_{\text{el}} = 1 - \Phi_{\text{en}}$. The efficiencies of energy and electron transfer, Φ_{en} and Φ_{el} , are defined as the proportion of $^3\text{NN}^* \cdot \text{CAR}$ quenching encounters that yield $^3\text{CAR}^*$ and $\text{CAR}^{\cdot+}$, respectively. From kinetic absorption measurements in absence and presence of carotenoid and using the data in Table 1 with appropriate corrections²⁴ for incomplete scavenging of $^3\text{NN}^*$ by CAR and decay of $^3\text{CAR}^*$ during its formation, it is found that, for 77DH, $\Phi_{\text{en}} = 1.0$ and 0.7 and, for SEPT, $\Phi_{\text{en}} = 1.0$ and 0.6 in hexane and methanol, respectively. With the assumption that electron transfer, followed by separation into free ions, is the only other possible pathway for quenching then, for 77DH, $\Phi_{\text{el}} = 0.0$ and 0.3 and, for SEPT, $\Phi_{\text{el}} = 0.0$ and 0.4 in hexane and methanol, respectively. Taking into consideration the uncertainties in the photophysical parameters used to calculate them (see Table 1), these efficiencies are the same for both carotenoids. The molecular and environmental factors controlling the electron transfer yield in these systems will be the subject of future work involving a greater range of carotenoids and will be reported separately.

2. Resonance Raman Spectra. In general, the bands observed in carotenoid resonance Raman spectra are associated with the conjugated polyene backbone chain, the precise band positions being dependent on C=C and C—C bond orders which are influenced by the π -electron distribution. Theoretical calculations²⁰ based on Huckel and PPP methods have been used to provide structural information concerning bond lengths and bond orders in carotenoid ground states, triplet states, and radical ions. In addition, these calculations have been used to explain

(20) Lafferty, J.; Roach, A. C.; Sinclair, R. S.; Truscott, T. G.; Land, E. *J. Chem. Soc., Faraday Trans 1* **1977**, 73, 416.

(21) Kemula, W.; Sioda, R. *Naturwissenschaften* **1963**, 23, 708.

(22) Wilkinson, F. *Photoinduced Electron Transfer*; Fox, M. A., Chanon, M., Eds.; Elsevier: Amsterdam, 1988; Part A, p 207.

(23) Baird, N. C.; West, R. M. *J. Am. Chem. Soc.* **1971**, 93, 18.

(24) Bensasson, R.; Land, E. *J. Photochemical and Photobiological Reviews*; Smith, K. C., Ed.; Plenum: London, 1978; p 163.

Table 1. Photophysical Properties of 1-Nitronaphthalene (NN), 7,7-Dihydro- β -carotene (77DH), and Septapreno- β -carotene (SEPT)

	NN			77DH		SEPT	
	methanol	benzene	hexane	methanol	hexane	methanol	hexane
$\tau_T/\mu\text{s}$ ($\pm 15\%$)	12	5.7	1.1	13	10	8	7
$\lambda_{\text{max}}/\text{nm}$	590	585	550	476	476	480	475
Γ/cm^{-1} ^a	3840	4805	3175	780	694	1790	1730
$\epsilon_T/\text{dm}^3 \text{ mol}^{-1} \text{ cm}^{-1}$ ($\pm 20\%$)	8700 ^c	6900 ^b	10500 ^c	374000 ^e	420000 ^d	227000 ^f	235000 ^f

^a Absorption bandwidth at $\epsilon_T/2$. ^b Obtained by the energy transfer method using pulse radiolysis with biphenyl (0.1 mol dm^{-3}) as donor, for which $\epsilon_T = 27100 \text{ dm}^3 \text{ mol}^{-1} \text{ cm}^{-1}$ at 359 nm in benzene,²⁴ and a NN concentration of $10^{-3} \text{ mol dm}^{-3}$. ^c Relative to ϵ_T for $^3\text{NN}^*$ in benzene using a ratio of Γ values and assuming a solvent independent oscillator strength. ^d From ref 24. ^e Relative to ϵ_T in hexane using a ratio of Γ values and assuming a solvent independent oscillator strength. ^f Relative to ϵ_T in benzene²⁴ ($206000 \text{ dm}^3 \text{ mol}^{-1} \text{ cm}^{-1}$, $\Gamma = 1970 \text{ cm}^{-1}$) using a ratio of Γ values and assuming a solvent independent oscillator strength.

the observed differences in the ground state, triplet state, and radical cation UV-vis absorption spectra. In the neutral ground state of the carotenoids these theoretical models²⁰ predict regular and even C=C-C bond alternation in agreement with experimental observations. Consequently, the strongest bands observed in the resonance Raman spectrum of, for example, β -carotene ground state appear around 1520 and 1150 cm^{-1} and are assigned to C=C and C-C in-phase stretching modes, respectively.

In the carotenoid triplet state, theoretical models^{20,23} suggest a collapse of the regular bond alternation due to regions of intermediate bond character toward the ends of the polyene chain. This effect causes the bond alternation in the central region of the molecule to be out of step with that toward the ends, producing a reversal of the bond order in the central part of the polyene chain. Thus, in the case of β -carotene, the central bond (15, 15') in the ground state is a double bond, while in the triplet state, it is a single bond. Consequently, the resonance Raman spectra of carotenoid triplet states exhibit additional bands and different intensity profiles (see below) compared to those of the respective ground state spectra.¹⁶

For the carotenoid radical cations, theoretical models²⁰ indicate that regular bond alternation is largely preserved, although the bond alternation is predicted to be less pronounced toward the center of the polyene chain. On this basis, the appearance of the radical cation resonance Raman spectra is not expected to differ dramatically from the spectra of the parent molecules.

Prior to discussion of the individual resonance Raman spectra, it is important to note the difference in electronic structure of 77DH compared with SEPT. The rather unusual feature with respect to 77DH is that it possesses an even number ($n = 8$) of conjugated double bonds in contrast to SEPT ($n = 9$), β -carotene ($n = 11$), and other common carotenoids which possess an odd number of conjugated double bonds. The immediate consequence of this is that the central bond of the polyene chain in the 77DH ground state is a single bond and not a double bond as is the case for SEPT and β -carotene. Similarly, the bond order reversal in the triplet state, as discussed above, results in the central bond being a double bond in $^377\text{DH}^*$ and not a single bond as for $^3\text{SEPT}^*$. This difference is reflected in the observed resonance Raman spectra discussed below.

The resonance Raman spectra of the ground state, triplet state, and radical cation of 77DH and SEPT in methanol are shown in Figures 5 and 6, respectively. Note that the resonance Raman spectra of the triplet state and radical cation of both carotenoids were obtained by tuning the probe wavelength (485 and 760 nm, respectively) to the absorption band of the transient being investigated. Ground state and radical cation spectra in detergent micelles are shown in Figures 7 and 8, and the band positions and assignments for all spectra are given in Table 2. The poorer signal to noise ratio of the radical cation resonance Raman spectra relative to the ground and triplet state spectra is

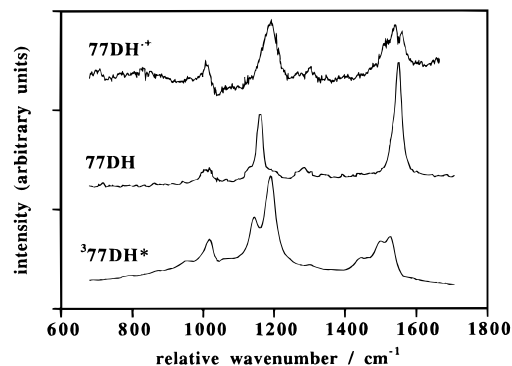


Figure 5. Resonance Raman spectra of the ground state, triplet state, and radical cation of 77DH in methanol. The triplet state of 77DH was sensitized by 355 nm excitation of a solution containing anthracene ($5 \times 10^{-5} \text{ mol dm}^{-3}$) and 77DH ($2 \times 10^{-5} \text{ mol dm}^{-3}$). The resonance Raman spectrum of $^377\text{DH}^*$ was obtained using a probe wavelength of 485 nm delayed 2 μs relative to the 355 nm excitation pulse. The 77DH radical cation was sensitized by 388 nm excitation of a solution containing 1-nitronaphthalene ($\sim 10^{-3} \text{ mol dm}^{-3}$) and 77DH ($2 \times 10^{-5} \text{ mol dm}^{-3}$), and the resonance Raman spectrum was obtained using a probe wavelength of 760 nm with a 2 μs delay. A probe only background has been subtracted from the original triplet state and radical cation pump/probe spectra. The ground state spectrum is solvent-subtracted.

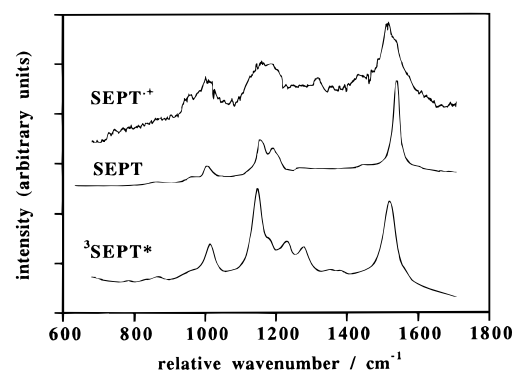


Figure 6. Resonance Raman spectra of the ground state, triplet state, and radical cation of SEPT in methanol. The experimental conditions were the same as those given for 77DH in the legend to Figure 5. The triplet and radical spectra were obtained by subtracting a probe only background from the pump/probe spectrum. The ground state spectrum is solvent-subtracted.

a consequence of the falloff in the efficiencies of the spectrograph and detector in the near-infrared region. As the resonance Raman spectra are similar in both methanol and TX-100 micelles, the following discussion of the methanol spectra applies equally well to the spectra in detergent micelles.

Both ground state spectra exhibit similarities with the resonance Raman spectrum of β -carotene reported previously.¹⁶ The most intense bands appear at 1551 and 1540 cm^{-1} for 77DH and SEPT, respectively, and are assigned to C=C stretching

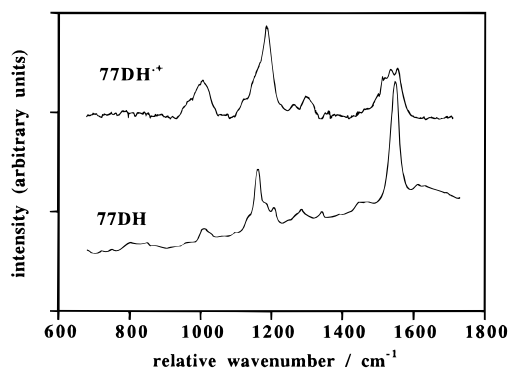


Figure 7. Resonance Raman spectra of the ground state and radical cation of 77DH in 2% Triton X-100. Both spectra were collected for 17 min, and the experimental conditions were as given in the legend to Figure 5. The radical spectrum was obtained by subtracting a probe only background from the pump/probe spectrum. The ground state spectrum is solvent-subtracted.

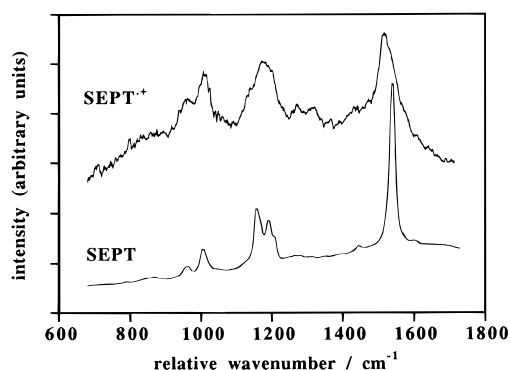


Figure 8. Resonance Raman spectra of the ground state and radical cation of SEPT in Triton X-100. Both spectra were collected for 17 min, and the experimental conditions were as given in the legend to Figure 5. The radical spectrum was obtained by subtracting a probe only background from the pump/probe spectrum. The ground state spectrum is solvent-subtracted.

modes. The difference in the positions of the C=C stretching bands between SEPT and 77DH reflects the longer conjugated chain length in SEPT relative to 77DH (cf. in β -carotene the band due to C=C stretching modes appears at ~ 1520 cm^{-1}). The bands between 1100 and 1200 cm^{-1} in both spectra are associated with C-C stretching modes but may contain contributions from C-H in-plane bending.¹⁴ In the case of SEPT, two bands appear in the C-C stretch region, one of medium intensity at 1155 cm^{-1} and another weaker band at 1191 cm^{-1} . In contrast, the resonance Raman spectrum of 77DH in this region shows a single strong band at 1162 cm^{-1} , although there is evidence of weaker bands on either side of

this band. The appearance of a single, dominant Raman band in the C-C stretch region of the 77DH spectrum may be due to the vibration of the central C-C bond that is not possible for SEPT. In both ground state spectra there is a weak band at ~ 1010 cm^{-1} that is associated with rocking of the methyl groups attached to the polyene chain.¹⁴ The band at 1274 cm^{-1} in the 77DH spectrum which is not present in the SEPT spectrum is assigned to a C-H in-plane bending mode that is not coupled with C-C stretching modes. There is no evidence of a similar band in the SEPT resonance Raman spectrum reflecting, perhaps, effective coupling of the C-C stretching modes with the in-plane C-H bending mode as suggested previously¹⁴ for ground state β -carotene.

The triplet state resonance Raman spectra of 77DH and SEPT (see Figures 5 and 6) in methanol display marked differences to the respective ground state spectra, which is consistent with previous observations in resonance Raman studies of other carotenoids.¹⁶ However, the most striking observation is the difference between the ${}^377\text{DH}^*$ and ${}^3\text{SEPT}^*$ spectra which contrasts with the relative similarity of the ground state spectra. Indeed, the resonance Raman spectrum of ${}^377\text{DH}^*$ contrasts markedly with the resonance Raman spectra of carotenoid triplets reported previously¹⁶ which, by and large, exhibit band profiles very similar to ${}^3\text{SEPT}^*$. Perhaps the most prominent feature of the ${}^377\text{DH}^*$ spectrum is in the C=C region where the strong single peak observed in the ground state spectrum is replaced by a group of three overlapping bands, all lying at lower wavenumber relative to the ground state C=C band. In contrast, the band due to the C=C stretch in the ${}^3\text{SEPT}^*$ spectrum (and the spectra of other carotenoid triplet states¹⁴) remains a single peak, shifted to lower wavenumber (1521 cm^{-1}) relative to the ground state band. The downward shift of 19 cm^{-1} for the C=C band in the ${}^3\text{SEPT}^*$ spectrum is similar in magnitude to the shifts reported for other carotenoids and reflects the decrease in bond order following promotion of an electron from a bonding MO to an antibonding MO. The origin of the triple-band system exhibited by ${}^377\text{DH}^*$ in the C=C stretch region is unclear but may be due to specific resonance enhancement of different C=C modes associated with regions of varying bond order as described above. In the C-C stretch region (1100–1200 cm^{-1}) the band profiles are again quite different for the two triplet states. In the case of ${}^377\text{DH}^*$, two bands (1191 and 1145 cm^{-1}) are observed in this region in contrast to the single band observed in the ground state spectrum. The stronger band at 1191 cm^{-1} is shifted upward by ~ 30 cm^{-1} relative to the ground state band, while the weaker band at 1145 cm^{-1} is 17 cm^{-1} lower than the ground state band. These two bands possibly arise from different resonantly enhanced C-C stretching modes as a consequence of the range of C-C bond strengths in the triplet state. It is interesting to note that the

Table 2. Resonance Raman Spectral Band Positions (in cm^{-1}) in Methanol and Micellar Solution

7,7'-dihydro- β -carotene			septapreno- β -carotene				assignment			
methanol		micelles	methanol		micelles					
77DH	${}^377\text{DH}^*$	77DH $^{+\bullet}$	77DH	77DH $^{+\bullet}$	SEPT	${}^3\text{SEPT}^*$	SEPT $^{+\bullet}$	SEPT	SEPT $^{+\bullet}$	
1009	1018	1009	961 1010	1005	963 1008	1014	957 1008	960 1008	955 1007	C-H out-of-plane deformation or CH ₃ rocking
1162	1145 1191	1188	1134 1162	1162 1188	1155 1191	1148 1190	1132 1173	1156 1192	1132 1178	C-C stretch
1274		1287 1303	1208 1282	1265 1298		1230 1279	1269 1442	1209 1428	1309 1428	C-H in-plane bending or CH ₃ deformation
1551	1449 1502 1529	1514 1541 1563	1548	1516 1537 1558	1540	1521	1517 1536	1539	1515 1528	C=C stretch

$^377\text{DH}^*$ spectrum shows little evidence of the band around 1240 cm^{-1} , found in other carotenoid triplet spectra,¹⁴ that is attributed to decoupled C–H in-plane bending. For $^3\text{SEPT}^*$, four Raman bands are observed in the $1100\text{--}1300\text{ cm}^{-1}$ region at 1148 (s) , 1190 (sh) , 1230 (m) , and $1279\text{ (m)}\text{ cm}^{-1}$ that exhibit a profile similar to carotenoid triplet spectra reported previously.¹⁶ The bands at 1148 and 1190 cm^{-1} are assigned to C–C stretching modes, while the band at 1230 cm^{-1} is assigned to C–H in-plane bending. The band at 1279 cm^{-1} is attributed to deformations of the methyl groups attached to the polyene chain. In both triplet spectra, a band in the $1015\text{--}1020\text{ cm}^{-1}$ range is observed and is assigned, as in the ground state spectra, to rocking of the methyl groups attached to the polyene chain.

The resonance Raman spectra of the radical cations $77\text{DH}^{+\bullet}$ and $\text{SEPT}^{+\bullet}$ (see Figures 5 and 6 for spectra in methanol solution and Figures 7 and 8 for spectra in detergent micelles) are more similar to the respective ground state spectra than the triplet state spectra, reflecting less dramatic structural changes between the ground state and the radical cation. The C=C stretch band in the $\text{SEPT}^{+\bullet}$ spectrum appears at 1517 cm^{-1} , i.e. 23 cm^{-1} lower in wavenumber relative to the ground state spectrum, although there is evidence of a shoulder around 1535 cm^{-1} . This shift reflects the decrease in C=C bond order following loss of an electron from a bonding MO and a decrease in regular bond alternation, particularly near the center of the polyene chain. The C–C band at 1173 cm^{-1} shows evidence of a pair of unresolved peaks that are slightly higher in wavenumber than in the ground state, suggesting a shortening of the C–C bonds in the polyene chain. The bands at 1008 and 1269 cm^{-1} have equivalent assignments to analogous bands in the ground and triplet state spectra.

The resonance Raman spectrum of $77\text{DH}^{+\bullet}$ displays a triple-band system in the C=C stretch region similar to that of the $^377\text{DH}^*$ spectrum, although the intensity profile is different and the shifts are less pronounced. The C–C band at 1188 cm^{-1} is at higher wavenumber than the corresponding ground state band (1162 cm^{-1}), indicating a shift of 26 cm^{-1} and an increase in the C–C bond order. The differences in band shifts between $77\text{DH}^{+\bullet}$ and $\text{SEPT}^{+\bullet}$ for the C=C and C–C bands may be due to the difference in the character of the central bond of each radical. In $77\text{DH}^{+\bullet}$, the central bond is a single bond that possesses more double-bond character relative to the equivalent bond in the ground state and hence gives rise to a Raman band at higher wavenumber ($1162 \rightarrow 1188\text{ cm}^{-1}$). In $\text{SEPT}^{+\bullet}$, the

central bond is a double bond that possesses more single-bond character than the equivalent bond in the ground state and so exhibits a downward band shift from 1540 to 1517 cm^{-1} .

We are in the process of extending this work to include other carotenoids (including β -carotene) of varying conjugated chain length with odd and even numbers of conjugated double bonds.

Conclusions

The resonance Raman spectra of the ground state, triplet state, and radical cation of $7,7'$ -dihydro β -carotene (77DH) and septapreno- β -carotene (SEPT) are reported for the first time. The marked differences in band positions and intensities between the two sets of spectra have been discussed in terms of theoretical models and are attributed to differences in electronic structure arising from 77DH possessing an even number ($n = 8$) of conjugated double bonds rather than an odd number as in SEPT ($n = 9$). The resonance Raman spectrum of $^3\text{SEPT}^*$ is very similar to the resonance Raman spectra of other carotenoids reported previously while, in contrast, the spectrum of $^377\text{DH}^*$ is very different and displays an intensity profile not observed in other carotenoid triplet spectra.

The observation of photoinduced electron transfer from 77DH and SEPT to $^3\text{NN}^*$ in competition with exchange energy transfer in methanol and TX-100 micellar solutions has been described. In hexane, no free radical ions are observed and the efficiencies of energy transfer have been estimated as 100% for quenching of $^3\text{NN}^*$ by 77DH and SEPT . In methanol, the efficiencies of energy transfer from $^3\text{NN}^*$ to 77DH and SEPT are considerably less ($\sim 70\%$ and 60% , respectively) than in hexane due to competition from electron transfer quenching as evidenced by the formation of the carotenoid radical cations in this solvent. The influence of solvent polarity and the nature of the polyene on the efficiency of electron transfer is the subject of an ongoing investigation involving a greater range of carotenoids and solvents and will be reported separately in a future publication.

Acknowledgment. The authors are grateful to R. Goyal for preliminary set-up work, to E. J. Land for assistance with pulse radiolysis measurements, and to Hoffman-La Roche and the Engineering and Physical Sciences Research Council (EPSRC) for financial support. The Raman experiments were carried out at the Lasers for Science Facility, Rutherford Appleton Laboratory, CCLRC.

JA953181R